

DEVELOPMENT OF A BEAM PROFILE MONITOR USING A NITROGEN-MOLECULAR JET FOR THE J-PARC MR *

Y. Hashimoto[#], Y. Hori, T. Morimoto, T. Toyama, M. Uota, KEK/J-PARC, Tokai, Japan
 T. Fujisawa, T. Murakami, K. Noda, NIRS, Chiba, Japan
 D. Ohsawa, Kyoto University, Kyoto, Japan

Abstract

In order to measure a beam profile with a wide dynamic range covering the halo region around the core region of intense proton beams, a non-destructive beam profile monitor using a sheeted jet beam of nitrogen molecules as a target has been developed for the beam of the J-PARC main ring (MR). Two-dimensional detection of the beam core will be performed using de-excitation light of nitrogen molecule. On the other hand, beam halo will be detected using ionized electron. In the detection of the electron, a micro channel plate (MCP) will be used for charge multiplication. To achieve a sensitivity of about 10^{-6} , a phosphor screen will be employed for the anode of the MCP, and its light will be detected by photomultipliers array for position resolving. Thus beam core and halo will be detected simultaneously in this scheme. In this paper, two subjects working on now as below are described: (1) Examination of the method for measurement of the density distribution of nitrogen molecules in the sheeted target area, and (2) Method for background evaluation in halo detection.

simulation, when external parallel fields of ± 30 kV/ 75 mm in electric and 0.05 T in magnetic are applied for the electron collection, and when intense proton beams of MR are supposed, a position error of collected electron was 0.3 mm at the maximum.

EQUIPMENT OUTLINE

Figure 1 and 2 show conceptual schematic view for the equipment. We measure the de-excitation light of nitrogen molecules occurring by a collision with the beam core and the target of the jet, by using an optical system.

INTRODUCTION

This non-destructive profile monitor has a role of diagnose circulating proton beam in the high intensity proton synchrotron of MR with a high sensitivity. A collision with a sheeted jet target of nitrogen molecules with the circulating proton beam is used for the detection of the beam profile with two methods described in abstract.

Past developments are shown as below. For the methods, examination and principle demonstration of the technique were carried out so far [1, 2]. Further, by using these techniques together, a high sensitive profile monitor having a wide dynamic range of six orders was proposed [3]. As for the light signal from the beam core is feeble [2], a large acceptance optical system is required. Our some members developed such an optical system in the vacuum with big acceptance angle of 30 degrees for the high sensitive beam profile monitor using the multi-screen [4]. Even this monitor can use this. In addition, a radiation hardened image intensifier having two MCP stages to use for the de-excitation light detection has already developed [2] with HAMAMATSU. In case of electron collection in the beam halo region, the position error in electron collection was evaluated by a time transient simulation during bunch time. The result of the

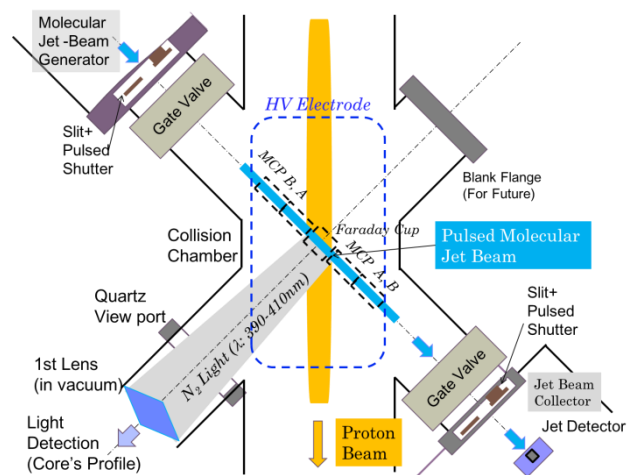


Figure 1: Horizontal cross-sectional schematic view of the collision point.

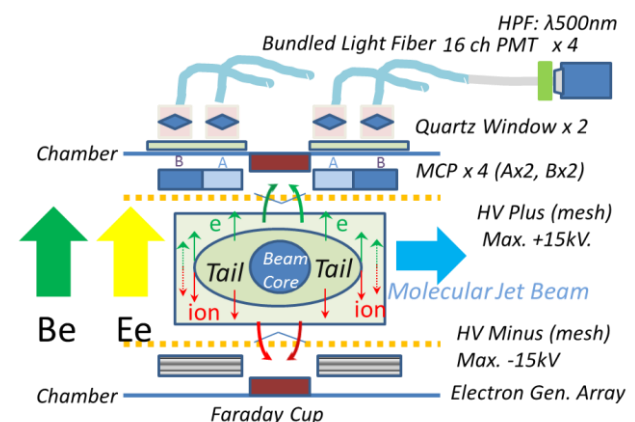


Figure 2: Vertical cross-sectional schematic view of the collision point.

*Work supported by MEXT/JSPS KAKENHI Grant Number 24310079 (Grant-in-Aid for Scientific Research(B))
[#]yoshinori.hashimoto@kek.jp

In addition, ionization electrons occurring by a collision in the halo region are amplified by using MCP. A phosphor screen for the MCP anode for high sensitivity detection is employed, and the light emitted from the screen is transferred to outside photo multiplier array (PMT's) via light fibers. Figure 3 shows sensitivity domain of the optical measurement and the electron measurement.

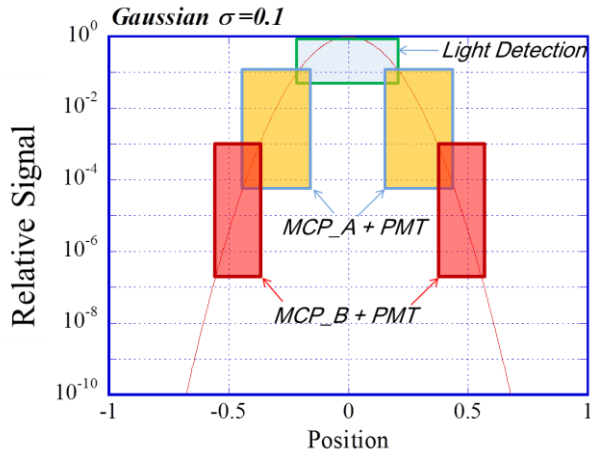


Figure 3: Dynamic range for universal Gaussian beam assumed bunch intensity of 2×10^{13} proton or higher, colored by detector segment.

DENSITY DISTRIBUTION OF NITROGEN MOLECULES IN THE TARGET

Table 1 shows the status of the jet beam generator. Figure 4 shows a photograph and the assembling drawing of the jet generator. The device consists of four differential evacuation chambers. In the figure, #1 is the nozzle chamber having the nozzle and the first skimmer, #2 is the second skimmer chamber having the second skimmer, and #3 is a slit chamber having a slit for shaping jet into a planer form. The measurement of the jet uses ionization gauge at the fourth (#4) chamber whose centre is equivalent to the collision point with the proton beam. Each chamber has turbo molecular pump of 500L/s. The sizes of the nozzle, of the skimmer, and of the slit are shown in Table 1. Because the skimmers and the slit located at chamber border, they have a role of orifice for differential pumping.

Table 1: Specification of the Jet Generator

Parameter	Value
Pulse Duration	100-1000 μ s
Source Pressure	1.0 MPa
Nozzle Size	1.83 mm dia.
1st/2nd Skimmer Size	$6.0^H \times 3.0^V / 20^H \times 5^V \text{ mm}^2$
Slit #3-4	$80^H \times 1.5^V \text{ mm}^2$

The design density of the jet target is more than 5×10^{-4} Pa equivalent, and the target sizes are $100 \times 100 \text{ mm}^2$. The design value of the target thickness is 1-3 mm. The setup of measurements of the jet is shown in Fig. 5.

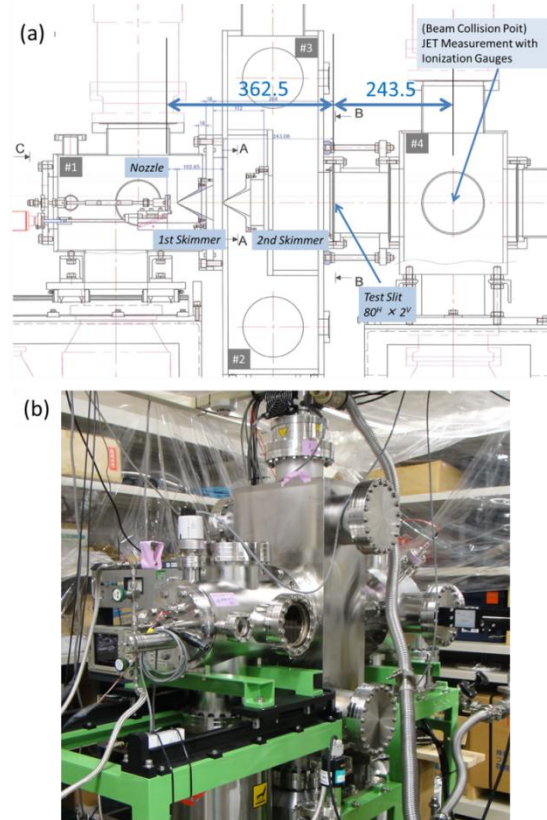


Figure 4: The jet generator. (a) assembling drawing, (b) a photo of our test bench.

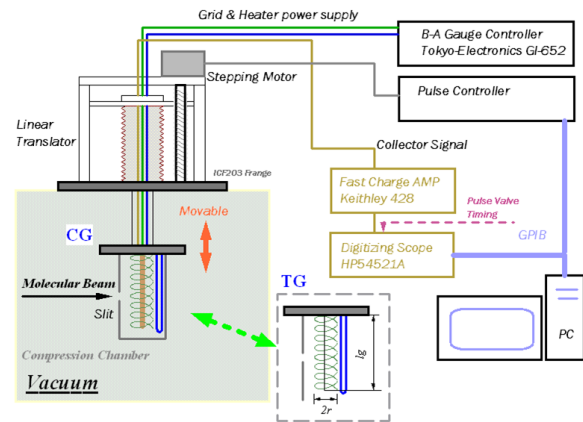


Figure 5: The setup for jet measurement with ionization gauges. CG: compression gauge, TG: thru gauge.

Two types of ionization gauge are used as below: (CG) compression gauge has a chamber with small slit at surroundings of the gauge, (TG) thru gauge has a slit in the surface of injection of the jet. The CG does time integration for pulsed jet beam. TG measures the pressure

of the jet at the time of the passage. Because the beams which passed TG are scattered in downstream chamber wall and come back, region of early 500 μ s of the pulse can be measured. TG and the CG are used properly depending on a purpose.

These gauges are attached to a linear actuator, and these gauges can scan space. They can be attached to both of horizontal and vertical directions at #4 chamber. The gauge output signal is measured with a high-speed current amplifier having rising time of 10 μ s (Keithley 428).

Results of the correlation of stagnation pressure and the jet pressure are shown in Fig. 6. The pressure of the jet increases as stagnation pressure rises, though the increase is almost saturated at 1 MPa.

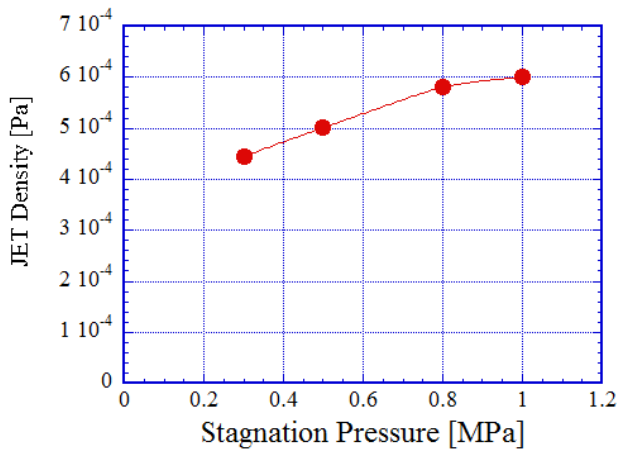


Figure 6: Correlation of the stagnation pressure and the jet pressure.

Figure 7 shows a vertical density distribution by the slit (#3-#4) width of 2 mm when stagnation pressure was 1.0 MPa. The width becomes 6.2 mm in FWHM in this profile. It might become around 3.5 mm by a slit of 2 mm geometrically, but larger than it. The reason is that this tail shows the scattering by the slit edges. In practical use, by using another one step, a slitting is necessary.

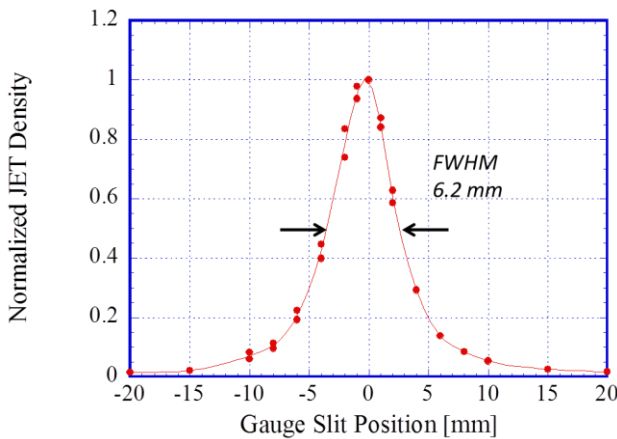


Figure 7: A vertical density distribution at #4 chamber.

Horizontal spatial distribution was measured in the region of ± 60 mm by CG with a step of 5 mm. All CG signal were taken 64 times of average (unevenness <3%). The CG signals were plotted in Fig. 8 only the part of its center ± 45 mm. Because CG output expresses integration of molecules inflow, when the slope is linear, it means constant inflow. In the figure, there is a good linearity region at 1.6 – 2.2 ms part. Values differentiated the CG signals of this region were plotted in Fig. 9 as colored contour map. This map expresses a density distribution of the jet plane at the collision region. Because the terminal velocity of the jet of nitrogen molecule is 730 mm/ms [5], then the time scale is converted into the length scale with this value. An enclosed region with black dashed line of the figure means $\pm 10\%$ non-uniform. The sizes of this region is understood the length of 90 mm of the line of the jet and the width of 80 mm. This region is a candidate for the collision target. In order to stretch the width, the aperture width of the second skimmer should be widened

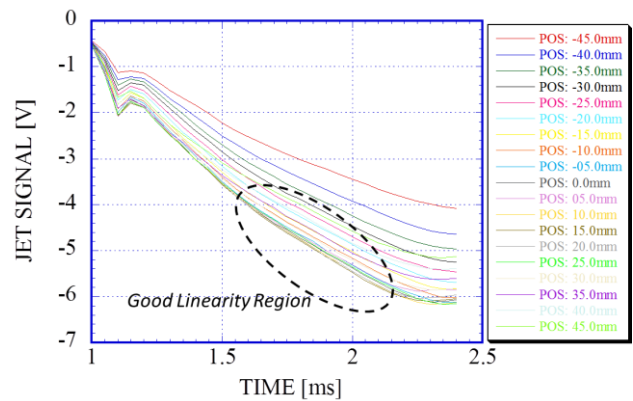


Figure 8: A various [H: -45,+45 mm] jet-pressure measured data by CG.

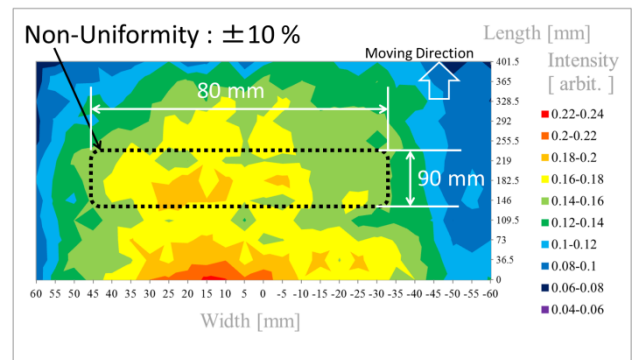


Figure 9: A contour map of jet density.

BACKGROUND EVALUATION

In the halo measurement to require high sensitivity, it is necessary to evaluate a noise to be carried on light signal.

At first scheme of the halo measurement as shown in Fig. 2 are discussed. In the method the ionization electrons produced by the collision in the beam tail region

are collected into the MCP's with the external fields of E_c and B_c , and then electrons are multiplied. At the anode of the MCP's phosphor screens are used to convert into monochromatic light. The converted lights are transferred with optical fibers, and then they are detected by PMT's. In this scheme, the reason of using monochromatic light is to reduce effects by external noise produced by beam loss. At the entrance of PMT, light filter for around 550 nm will be set for noise reduction.

Considering such an external noise, remarkable contribution is Cherenkov light by the second charged particle occurring in beam loss in visible light region. Cherenkov light is also used for beam loss detection, beam loss monitors using optical fiber was reviewed by T. Obina in this conference [6]. As for the number of produced photons per unit length per wave length of this light, come to next formula [6],

$$\frac{d^2N}{dx d\lambda} = \frac{2\pi\alpha}{\lambda^2} \left(1 - \frac{1}{\beta^2 n^2}\right)$$

where β : light velocity ratio, n : refractive index of medium, α : fine structural constant. The number of the emitted photons per 10 nm band width in a glass of 10 mm thickness is plotted in Fig. 10 [6]. From this, the light wavelength of the phosphor of MCP understands that one as long as possible is not affected by the Cherenkov light. For the phosphor, faster attenuation time is also required, the time should be within a bunch separation time of 600 ns. A candidate characteristics of the phosphor are the attenuation time is 300 ns (1/10) and its wavelength is 550 nm.

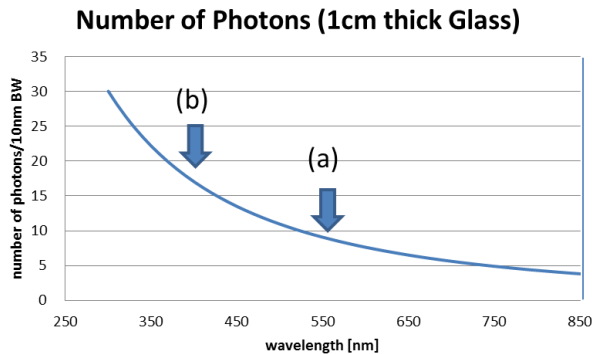


Figure 10: A calculated photon number in a glass [6].

For the background evaluation in MR, a test device is prepared as shown in Fig. 11. It has two kinds of MCP which put in the small vacuum container. These MCPs specifications are bellows: (a) the candidate predicted above, (b) wavelength: 400 nm, the attenuation time: 80 ns. Because the Cherenkov occurs at beam time, when type of (a) of MCP is used, there is a method for avoiding external lights that a gated detection is possible at the time of after bunch time. The light signal is transferred to the PMTs via optical fiber, and then external noise derived from beam loss is also evaluated.

The radiation of the proposed test site in MR was already measured. A result of dose per week was around 50 mGy during continuous accelerator operation with beam power of 220 kW.

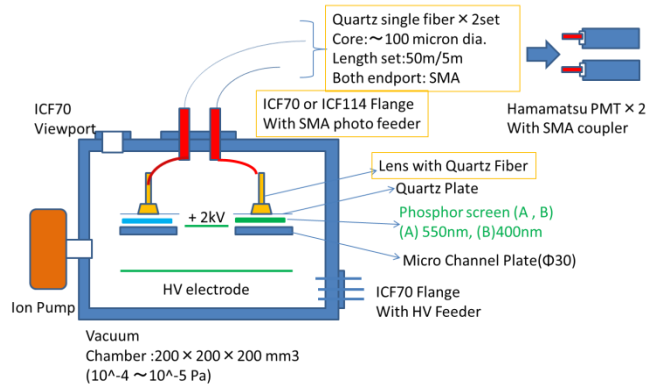


Figure 11: A test device for background evaluation.

SUMMARY AND PROSPECTS

An evaluation for the uniformity of the jet target was carried out. The measurement of the characteristics of intense jet beams is studying continuously, and the uniformity evaluation should be more reliable.

In addition, a sensitive actual background test will be planned in MR tunnel for beam halo detection.

With the goal of installing it in the next fiscal year, the practical designing for the collision chamber, for the electronic collection electrode, and for the optical system to measure the beam core are scheduled this autumn.

Finally the authors are grateful to T. Obina (KEK) for lecturing on optical fiber based beam loss monitor and giving us useful data. We would like to also thank H. Saito of company SEIWA for fabrication of the jet generator. We also appreciate the help received from H. Akino, Y. Omori, T. Kawachi, and S. Otsu of Mitsubishi Electric System & Service Co., Ltd..

REFERENCES

- [1] Y. Hashimoto, et al., NIM A 527 (2004) 289-300.
- [2] Y. Hashimoto, et al., Proc. of IPAC'10, Kyoto, Japan, p.789.
- [3] Y. Hashimoto, et al., Proc. of IBIC'12, Tsukuba, Japan, p.511.
- [4] Y. Hashimoto, et al., Proc. of IBIC 2013, Oxford, UK, TUCL2.
- [5] D. R. Miller, "Atomic and Molecular Beam Methods, Volume 1", Edited by Giacinto Scoles, New York, Oxford Press, (1988).
- [6] T. Obina, "Optical fiber based loss monitor for electron storage ring", Proc. of IBIC 2013, Oxford, UK, WECL1.